Raman Signature of the Fe_2O_2 "Diamond" Core

Elizabeth C. Wilkinson,[1a] Yanhong Dong,[1a] Yan Zang,[1a] Hiroshi Fujii,[1a] Robert Fraczkiewicz,[1b] Grazyna Fraczkiewicz,[1b] Roman S. Czernuszewicz,*[,1b] and Lawrence Que, Jr.*[,1a]

Contribution from the Department of Chemistry and Center for Metals in Biocatalysis, University of Minnesota, Minneapolis, Minnesota 55455, and Department of Chemistry, University of Houston, Houston, Texas 77204

Received September 12, 1997

Abstract: We report the resonance Raman (RR) spectra of iron complexes containing the $Fe_2(\mu\text{-}O)_2$ core. Frozen CH_3CN solutions of the $Fe^{III}Fe^{IV}$ intermediate $[Fe_2(\mu\text{-}O)_2L_2](ClO_4)_3$ (where L = TPA, 5-Me_3-TPA, 5-Me_2-TPA, 5-MeTPA, 5-Et_3-TPA, or 3-Me_3-TPA) show numerous resonance-enhanced vibrations, and among these, an oxygen-isotope-sensitive vibration around 667 cm^{-1} that shifts ca. 30 cm^{-1} when the samples are allowed to exchange with $^{18}OH_2$, and whose Raman shift does not vary with methyl substitution of the TPA ligand. Spectra of iron-isotope-substituted samples of $[Fe_2(\mu\text{-}O)_2(L)_2](ClO_4)_3$ (^{54}Fe and ^{57}Fe for L = TPA, and ^{54}Fe and ^{58}Fe for L = 5-Me_3-TPA) show that this vibration is also iron-isotope-sensitive. These isotopic data taken together strongly suggest that this vibration involves motion of the $Fe_2(\mu\text{-}O)_2$ core that is isolated from motions of the ligand. A frozen CH_3CN solution of the diiron(III) complex $[Fe_2(\mu\text{-}O)_2(6\text{-}Me_3\text{-}TPA)_2](ClO_4)_2$ shows one intense resonance-enhanced vibration at 692 cm^{-1} that shifts −30 cm^{-1} with ^{18}O labeling. Normal coordinate analysis of the $Fe_2(\mu\text{-}O)_2$ core in $[Fe_2(\mu\text{-}O)_2(5\text{-}Me_3\text{-}TPA)_2](ClO_4)_3$ supports the assignment of the Fermi doublet centered around 666.2 cm^{-1} as an A_1 vibration of this core. Furthermore, we propose that this unique feature found in the region between 650 and 700 cm^{-1} is indicative of a diamond core structure and is the Raman signature of an iron cluster containing this core.

Introduction

The $M_2(\mu\text{-}O)_2$ diamond core has recently emerged as a common feature in the high-valent chemistry of a number of first-row transition metals. Complexes with such cores are now characterized for Mn,[2] Fe,[3] and Cu,[4] and serve as synthetic precedents for the $M_2(\mu\text{-}O)_2$ diamond core in corresponding metalloenzymes. There is a large number of crystallographically defined complexes with the $Mn_2(\mu\text{-}O)_2$ core, representing the $Mn^{III}Mn^{III}$, $Mn^{III}Mn^{IV}$, and $Mn^{IV}Mn^{IV}$ oxidation states.[2] All evidence points to the $Mn_2(\mu\text{-}O)_2$ core as present in an inactive superoxidized form of manganese catalase[5] and, more importantly, as the basic structural motif in the various S states of the oxygen-evolving complex in photosystem II.[6] However, only recently have iron[3] and copper[4] complexes with the $M_2(\mu\text{-}O)_2$ diamond core been prepared and characterized. Their remarkable structural, spectroscopic, and reactivity properties serve as the foundation for the hypothesis that such cores may participate in the high-valent chemistry of dioxygen-activating iron and copper enzymes such as methane monooxygenase, ribonucleotide reductase, and tyrosinase.[7,8] Indeed, evidence suggesting such an Fe_2O_2 core has just been reported for the high-valent intermediate Q in the methane monooxygenase cycle.[9] Finally, the recent demonstration that the $M_2(\mu\text{-}O)_2$ diamond core can be in equilibrium with the isomeric $M_2(\mu\text{-}\eta^2\text{:}\eta^2\text{-}O_2)$ core in the Cu(^{i}Pr$_3$TACN) system[8a,10] potentially unites the oxygen activation chemistry of Fe and Cu enzymes and the water oxidation chemistry of Mn in the photosynthetic apparatus into a common mechanistic framework for oxygen chemistry at nonheme dinuclear metal centers.

As deduced from X-ray crystallography,[2−4] the principal features of the $M_2(\mu\text{-}O)_2$ diamond core are its short metal−oxo bonds (ca. 1.8 Å), its acute M−O−M angles (90−110°), and a metal−metal separation of less than 3 Å. In the absence of suitable crystals, evidence for such cores can also be obtained

(1) (a) University of Minnesota. (b) University of Houston.

(2) Manchanda, R.; Brudvig, G. W.; Crabtree, R. H. *Coord. Chem. Rev.* **1995**, *144*, 1−38.

(3) (a) Zang, Y.; Dong, Y.; Que, L., Jr. *J. Am. Chem. Soc.* **1995**, *117*, 1169−1170. (b) Dong, Y.; Fujii, H.; Hendrich, M. P.; Leising, R. A.; Pan, G.; Randall, C. R.; Wilkinson, E. C.; Zang, Y.; Que, L., Jr.; Fox, B. G.; Kauffmann, K.; Münck, E. *J. Am. Chem. Soc.* **1995**, *117*, 2778−2792. (c) Dong, Y.; Que, L., Jr.; Kauffmann, K.; Münck, E. *J. Am. Chem. Soc.* **1995**, *117*, 11377−11378.

(4) (a) Mahapatra, S.; Halfen, J. A.; Wilkinson, E. C.; Pan, G.; Wang, X.; Young, V. G., Jr.; Cramer, C. J.; Que, L., Jr.; Tolman, W. B. *J. Am. Chem. Soc.* **1996**, *118*, 11555−11574. (b) Mahapatra, S.; Young, V. G., Jr.; Kaderli, S.; Zuberbühler, A. D.; Tolman, W. B. *Angew. Chem., Int. Ed. Engl.* **1997**, *36*, 111−113.

(5) (a) Waldo, G. S.; Yu, S.; Penner-Hahn, J. E. *J. Am. Chem. Soc.* **1992**, *114*, 5869−5870. (b) Dismukes, G. C. In *Bioinorganic Catalysis*; Reedjik, J., Ed.; Marcel Dekker: Amsterdam, 1992; pp 317−346. (c) Gamelin, D. R.; Kirk, M. L.; Stemmler, T. L.; Pal, S.; Armstrong, W. H.; Penner-Hahn, J. E.; Solomon, E. I. *J. Am. Chem. Soc.* **1994**, *116*, 2392−2399.

(6) (a) Kirby, J. A.; Robertson, A. S.; Smith, J. P.; Thompson, A. C.; Cooper, S. R.; Klein, M. P. *J. Am. Chem. Soc.* **1981**, *103*, 5529−5537. (b) Yachandra, V. K.; DeRose, V. J.; Latimer, M. J.; Mukerji, I.; Sauer, K.; Klein, M. P. *Science* **1993**, *260*, 675−679. (c) Yachandra, V. K.; Sauer, K.; Klein, M. P. *Chem. Rev.* **1996**, 2927−2950.

(7) Que, L., Jr.; Dong, Y. *Acc. Chem. Res.* **1996**, *29*, 190−196.

(8) (a) Halfen, J. A.; Mahapatra, S.; Wilkinson, E. C.; Kaderli, S.; Young, V., Jr.; Que, L., Jr.; Zuberbühler, A. D.; Tolman, W. B. *Science* **1996**, *271*, 1397−1400. (b) Solomon, E. I.; Sundaram, U. M.; Machonkin, T. E. *Chem. Rev.* **1996**, *96*, 2563−2605.

(9) Shu, L.; Nesheim, J. C.; Kauffmann, K.; Münck, E.; Lipscomb, J. D.; Que, L., Jr. *Science* **1997**, *275*, 515−518.

(10) Abbreviations used: N5, *N*-(hydroxyethyl)-*N*,*N*′,*N*′-tris(2-benzimidazolylmethyl)-1,2-diaminoethane; R_3TACN, 1,4,7-trialkyl-1,4,7-triazacyclononane; TPA, tris(2-pyridylmethyl)amine; modifiers preceding TPA denote the position of the alkyl substituent on the pyridine ring and the number of rings modified.

S0002-7863(97)03220-4 CCC: $15.00
Published on Web 01/27/1998

from X-ray absorption spectroscopy, EXAFS in particular. Due to its rigidity, the $M_2(\mu\text{-}O)_2$ diamond core exhibits a prominent feature at ca. 2.7 Å in the Fourier-transformed spectrum due to the scattering from the other metal center.[3b,4a,6a,8a] This short metal−metal distance together with appropriately short metal−oxygen bond lengths provides strong support for the $M_2(\mu\text{-}O)_2$ diamond core. Indeed the EXAFS technique has proven useful for establishing the presence of such cores in manganese catalase,[5] the photosynthetic oxygen-evolving complex,[6] and intermediate Q of methane monoxygenase.[9]

Resonance Raman spectroscopy is yet another spectroscopic tool for probing the $M_2(\mu\text{-}O)_2$ diamond core. Due to its novel geometry, vibrations unique to this core may be observed and serve as diagnostic features for the presence of such centers in synthetic reaction mixtures and metalloenzyme intermediates. Studies thus far show that there is an intense resonance-enhanced vibration in the 600−700 cm^{-1} region in the spectra of synthetic Mn,[11] Fe,[3b] and Cu[4] complexes. In this paper, we report a resonance Raman analysis of complexes with the $Fe_2(\mu\text{-}O)_2$ diamond core using Fe, O, and N isotope substitution and ligand modification. With the available isotopic substitution data, we have carried out a normal coordinate analysis for the $Fe_2(\mu\text{-}O)_2$ core in $[Fe_2(\mu\text{-}O)_2(L)_2]^{3+}$ (L = TPA and its methyl-substituted derivatives) and assign the nature of the unique vibration in the 600−700 cm^{-1} region that is the Raman "signature" for this diamond core.

Results and Discussion

Geometric Features of the $Fe_2(\mu\text{-}O)_2$ Diamond Core. The complex $[Fe_2(\mu\text{-}O)_2(6\text{-}Me_3\text{-}TPA)_2](ClO_4)_2$ (**1**) is the first and only Fe_2O_2 complex to be crystallographically characterized to date[3a] and as such provides important structural parameters for the vibrational analysis of other Fe_2O_2 complexes whose crystal structures are not yet available. The X-ray structure of **1** shows an $Fe_2(\mu\text{-}O)_2$ core with C_{2h} symmetry, with geometric features detailed in Figure 1. This novel structure exhibits an Fe−O−Fe angle of 92.5°, significantly smaller than found for any other (μ-oxo)diiron(III) structure as required by the diamond core; indeed such small angles are present in related $M_2(\mu\text{-}O)_2$ complexes (92−102°). Furthermore there is a difference of nearly 0.08 Å between the two Fe−μ-O components of each Fe−O−Fe unit. For comparison, the structure of the related $[Cu_2(\mu\text{-}O)_2(d_{21}\text{-}Bn_3TACN)_2]^{2+}$ complex shows a $Cu_2(\mu\text{-}O)_2$ core with nearly D_{2h} symmetry, with Cu−O bond lengths differing only by 0.005 Å, while for $Mn^{III}Mn^{III}$ and $Mn^{IV}Mn^{IV}$ complexes with $Mn_2(\mu\text{-}O)_2$ cores, the Mn−O bond lengths are usually comparable in length but can differ by as much as 0.05 Å.[12] Notably the Fe_2O_2 core of $[Fe_2(\mu\text{-}O)_2(6\text{-}Me_3\text{-}TPA)_2](ClO_4)_2$ has the largest distortion toward C_{2h} symmetry observed. While the presence of different ligands *trans* to the oxo bridges can contribute to the bond length differences, it is clear from these structural comparisons that other factors yet unrecognized exacerbate the asymmetry of the M−O−M unit in the diiron complex.

The core structure of $[Fe_2(\mu\text{-}O)_2(5\text{-}Me_3\text{-}TPA)_2](ClO_4)_3$ (**2**) appears to exhibit a similar distortion toward C_{2h} symmetry, as shown in Figure 1c. While a crystal structure of this complex has not been obtained, this geometry is deduced from a body of spectroscopic data. On the basis of its EPR and Mössbauer properties, **2** is best described as a valence-delocalized low-spin Fe(III)−low-spin Fe(IV) complex; consequently the two metal sites are essentially identical. The diamond core structure is deduced from EXAFS analysis which requires an Fe−Fe distance of 2.89 Å. As with $[Fe_2(\mu\text{-}O)_2(6\text{-}Me_3\text{-}TPA)_2](ClO_4)_2$, the Fe−O−Fe unit has unequal bond lengths; one Fe−μ-O distance is 1.77 Å, while the other Fe−μ-O distance is included in a three-scatterer shell averaging 1.94 Å. DFT calculations[18] on $[Fe_2(\mu\text{-}O)_2(TPA)_2](ClO_4)_3$ predict Fe−μ-O bond lengths of 1.77 and 1.83 Å with an Fe−Fe distance of 2.83 Å, parameters in good agreement with the EXAFS results.

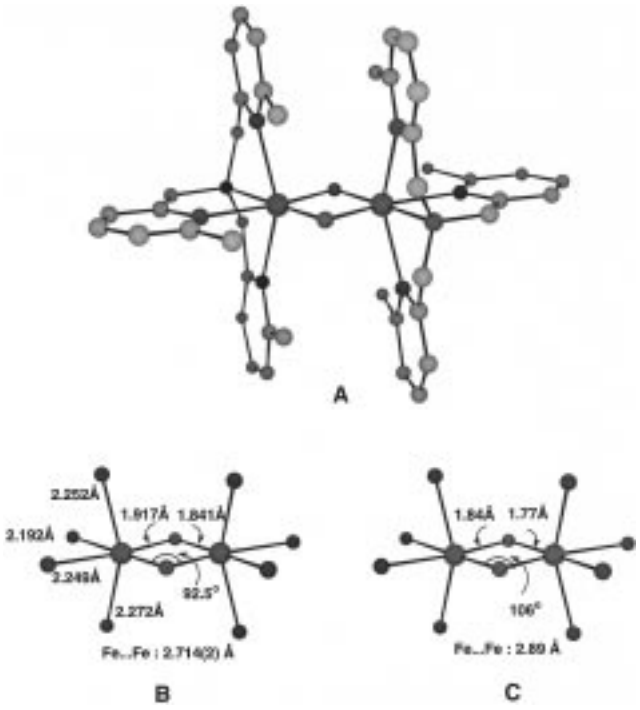

Figure 1. (A) Crystal structure of $[Fe_2(\mu\text{-}O)_2(6\text{-}Me_3\text{-}TPA)_2](ClO_4)_2$. (B) Parameters of the $Fe_2(\mu\text{-}O)_2$ core from the crystal structure of $[Fe_2(\mu\text{-}O)_2(6\text{-}Me_3\text{-}TPA)_2](ClO_4)_2$. (C) Proposed structure of $[Fe_2(\mu\text{-}O)_2(5\text{-}Me_3\text{-}TPA)_2](ClO_4)_3$ with distances derived from EXAFS DFT calculations, and angles calculated using simple trigonometric relationships.

[$Fe_2(\mu\text{-}O)_2$] Core Vibrations. The resonance Raman spectrum of a frozen CH_3CN solution of $[Fe^{III}_2(\mu\text{-}O)_2(6\text{-}Me_3\text{-}TPA)_2](ClO_4)_2$ derived from excitation into its visible absorption band at 500 nm shows an intense vibration at 692 cm^{-1} (Figure 2a). This is the only feature observed in the spectrum of **1**. The energy of this band is intermediate between those observed for heme Fe=O complexes (800−850 cm^{-1}) and those typically observed for (μ-oxo)diiron(III) complexes (450−550 cm^{-1}). If the sample is allowed to exchange with $H_2{}^{18}O$ at low temperature, one oxo group becomes protonated, resulting in the formation of $[Fe^{III}_2(\mu\text{-}O)(\mu\text{-}OH)(6\text{-}Me_3\text{-}TPA)_2](ClO_4)_3$, which is then deprotonated to re-form $[Fe^{III}_2(\mu\text{-}O)_2(6\text{-}Me_3\text{-}TPA)_2](ClO_4)_2$ (presumably with incorporation of ^{18}O label), isolated as a solid, and then redissolved in dry CH_3CN. The resonance Raman spectrum of a sample prepared in this manner (Figure 2b) shows a new feature at 660 cm^{-1}, resulting from incomplete exchange with $H_2{}^{18}O$,[13] in addition to the dominant feature at 692 cm^{-1}. Attempts to obtain samples of $[Fe^{III}_2(\mu\text{-}O)_2(6\text{-}Me_3\text{-}TPA)_2](ClO_4)_2$ containing a higher percentage of ^{18}O label were unsuccessful due to the sensitivity of the complex to water, resulting in its decomposition.

(11) Czernuszewicz, R. S.; Dave, B.; Rankin, J. G. In *Spectroscopy of Biological Molecules*; Hester, R. E., Girling, R. B., Eds.; Royal Society of Chemistry: Cambridge, 1991; pp 285−288.

(12) Goodson, P. A.; Oki, A. R.; Glerup, J.; Hodgson, D. J. *J. Am. Chem. Soc.* **1990**, *112*, 6248−6254.

(13) There is no evidence of a residual of $[Fe^{III}_2(\mu\text{-}O)(\mu\text{-}OH)(6\text{-}Me_3\text{-}TPA)_2](ClO_4)_3$ in the sample. This complex has a λ_{max} of 550 nm and a distinct peak at 676 cm^{-1} in its Raman spectrum that shifts to 646 cm^{-1} upon exchange with $H_2{}^{18}O$.

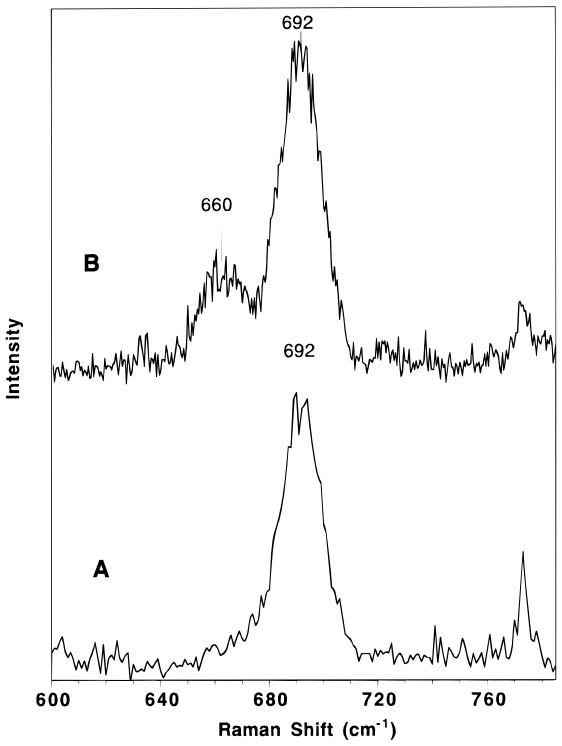

Figure 2. Resonance Raman spectra obtained with 457.9 nm excitation of a frozen CH_3CN solution of (A) $[Fe_2(\mu\text{-}O)_2(6\text{-}Me_3\text{-}TPA)_2](ClO_4)_2$ and (B) $[Fe_2(\mu\text{-}O)_2(6\text{-}Me_3\text{-}TPA)_2](ClO_4)_2$ with incorporation of ^{18}O.

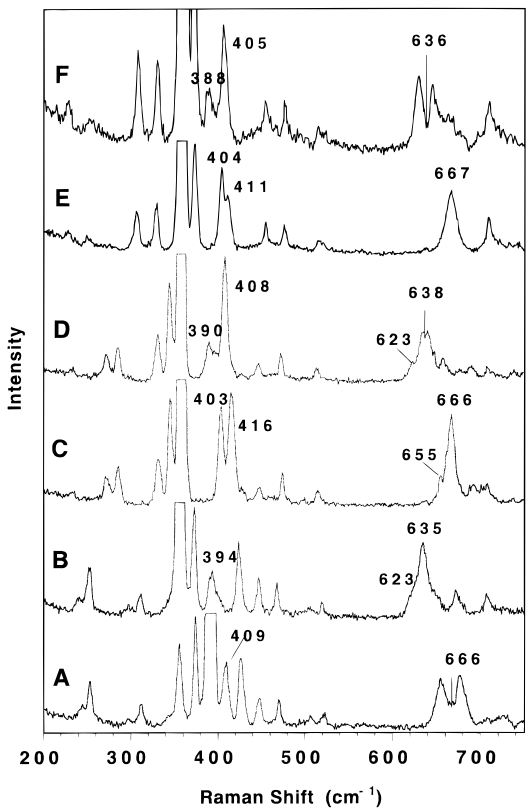

Figure 3. Resonance Raman spectra obtained with 613 nm excitation of frozen CH_3CN solutions of (A) $[Fe_2(\mu\text{-}O)_2(5\text{-}Me_3\text{-}TPA)_2](ClO_4)_3$, (B) $[Fe_2(\mu\text{-}^{18}O)_2(5\text{-}Me_3\text{-}TPA)_2](ClO_4)_3$ (sample is allowed to exchange with 100 equiv of of 98%-enriched $H_2{}^{18}O$ in solution at −40 °C), (C) $[Fe_2(\mu\text{-}O)_2(TPA)_2](ClO_4)_3$, (D) $[Fe_2(\mu\text{-}^{18}O)_2(TPA)_2](ClO_4)_3$), (E) $[Fe_2(\mu\text{-}O)_2(3\text{-}Me_3\text{-}TPA)_2](ClO_4)_3$, and (F) $[Fe_2(\mu\text{-}^{18}O)_2(3\text{-}Me_3\text{-}TPA)_2](ClO_4)_3$. These spectra were obtained at 1 cm^{-1} resolution.

The resonance Raman spectrum of the corresponding $[Fe^{III}\text{-}Fe^{IV}(\mu\text{-}O)_2(TPA)_2]^{3+}$ complex also exhibits an intense oxygen-isotope-sensitive vibration at 666.1 cm^{-1} but has a number of additional features to lower energy (Figure 3). To aid in assigning these features, we have prepared a series of $[Fe_2(\mu\text{-}O)_2(L)_2]^{3+}$ complexes where L is TPA or one of its 3-methyl- or 5-methyl-substituted derivatives. These complexes all show an intense visible absorption band at 616 nm, and excitation into this band with 613 nm laser light produces the resonance Raman spectra shown in Figure 3. These spectra show a gross pattern of features that are similar in Raman shift, intensity and sensitivity, to oxygen isotope substitution. The prominent vibrational features of this series (along with several other ligand variations) and the shifts upon exchange with $H_2{}^{18}O$ are summarized in Table 1. We have also prepared the following isotopically labeled complexes: $^{54}Fe/^{57}Fe$ for L = TPA and $^{54}Fe/^{58}Fe$ and $^{14}N/^{15}N$ at the tertiary amine position for L = 5-Me_3-TPA; the data are listed in Table 1.

The most striking common feature in these spectra is the prominent oxygen-isotope-sensitive band centered around 666 cm^{-1}. The sample where L = TPA shows a strongly resonance-enhanced vibration at 666.1 cm^{-1} that shifts to 637.9 with ^{18}O substitution. The 5-Me_3-TPA analogue exhibits a symmetric doublet centered at 666.2 cm^{-1}, which collapses to a single peak at 635 cm^{-1} upon exchange with $H_2{}^{18}O$. The 3-Me_3-TPA analogue, on the other hand, has a resonance-enhanced vibration at 667 cm^{-1}, which becomes a doublet centered at 636 cm^{-1} upon exchange with $H_2{}^{18}O$. The doublets observed in these spectra derive from Fermi resonance with ligand vibrations in the lower frequency region. Examination of this region identifies two vibrations which are suitable candidates for a combination band that could be in Fermi resonance with the ca. 666 cm^{-1} feature: 285 and 331 cm^{-1} for L = TPA, 312 and 356 cm^{-1} for L = 5-Me_3-TPA, and 306 and 329 cm^{-1} for L = 3-Me_3-TPA (Figure 3). These two fundamental ligand vibrations can combine to produce a band that has the correct energy and symmetry to interact with the 666 cm^{-1} vibration (Figure 4).[14] For L = TPA, the combination band would be found at 616 cm^{-1}—too low in energy to interact with the fundamental of either the ^{16}O or ^{18}O complex. For L = 5-Me_3-TPA, the combination band would be found at 668 cm^{-1}, which is close in energy to the fundamental of the ^{16}O complex, hence the Fermi doublet at that frequency. For L = 3-Me_3-TPA, the combination band would be found at 635 cm^{-1}—too low in energy to interact with the fundamental of the ^{16}O complex, but of the correct energy to interact with the fundamental of the ^{18}O complex. The ^{18}O complex where L = TPA shows a band centered at 637.9 cm^{-1} with weak splitting into nonresolved features at 633.9 and 641.9 cm^{-1}. The band centered at 637.9 cm^{-1} is too high in energy to be in Fermi resonance with the combination band that would be found at 616 cm^{-1}, but there is a weak band at 635 cm^{-1} (Figure 3c) that could be causing the observed splitting.

Because the frequency of the ca. 666 cm^{-1} vibration appears to be insensitive to the introduction of methyl groups on the TPA ligand, it must involve only motion of the $Fe_2(\mu\text{-}O)_2$ core which is isolated from motion of the tripodal ligand. The isotope shift for the ca. 666 cm^{-1} vibration is approximately 32 cm^{-1} for the five $[Fe_2(\mu\text{-}O)_2L_2](ClO_4)_3$ complexes with both oxo bridges ^{18}O-labeled (Table 1). These shifts correspond to those expected for a diatomic Fe−O stretch; however, more detailed ^{18}O-labeling experiments demonstrate that this vibration

(14) Cotton, F. A. *Chemical Applications of Group Theory*; Wiley-Interscience: New York, 1971; pp 330−333.

Table 1. Resonance Raman Data for $[Fe_2(\mu\text{-}O)L_2](ClO_4)_3$

L	isotope	oxygen-isotope-sensitive bands[a]				other bands[a]						
5-Me_3-TPA	^{16}O, ^{NA}Fe	676.7;655.7 (666.2)[b]		426.5	409.1	522(w)[c]	470	447	374	356	312(w)[c]	254
	^{18}O, ^{NA}Fe	635	623	426	394	521(w)	470	448	374	356	313(w)	253
	$^{18}O^{16}O$	not resolved			402							
	$^{15}N_{amine}$	no change										
	^{54}Fe	677.5, 656.7		428.5	410.1	522(w)	471	448	376	357	313(w)	254
	^{58}Fe	677.0, 652.3		422.5	403.9	521(w)	469	446	372	355	309(w)	254
5-Me_2-TPA	^{16}O	676, 664 (670)[b]		425	408				370(b)[d]		318(w)	
	^{18}O	632		420	392(b)				3709b)		318(w)	
5-Me-TPA	^{16}O	668		424	410			442	obs[e]	338(w)	322(w)	
	^{18}O	636		416	392(b)				364(b)	338(w)	322(w)	
TPA	^{16}O, ^{NA}Fe	666.1	655.3	416	403	514(w)	473	446	345	331	285 272(w)	254
	^{18}O, ^{NA}Fe	633.9, 641.9 (637.9)[b]	622.7	408	390	514(w)	473	446	345	331	285 272(w)	
	$^{18}O^{16}O$	644										
	^{54}Fe	667.0	654.4									
	^{54}Fe	663.3	651.2									
3-Me_3-TPA	^{16}O	667		411	404	515(w)	476	455	374	329	306	251(w) 228(w)
	^{18}O	644, 628 (636)[b]		405	388	514(w)	476	454	372	330	308	254(w) 228(w)

[a] Bands reported relative to the 922 cm^{-1} band of frozen CH_3CN or the 836 cm^{-1} band of frozen CD_3CN as internal standard. Bands with higher precision were derived from spectra obtained with a scan increment of 0.1 cm^{-1} as described in the Experimental Section. [b] Number in parentheses represents the center of the Fermi doublet. [c] w = weak. [d] b = broad. [e] obs = obscured by solvent peak.

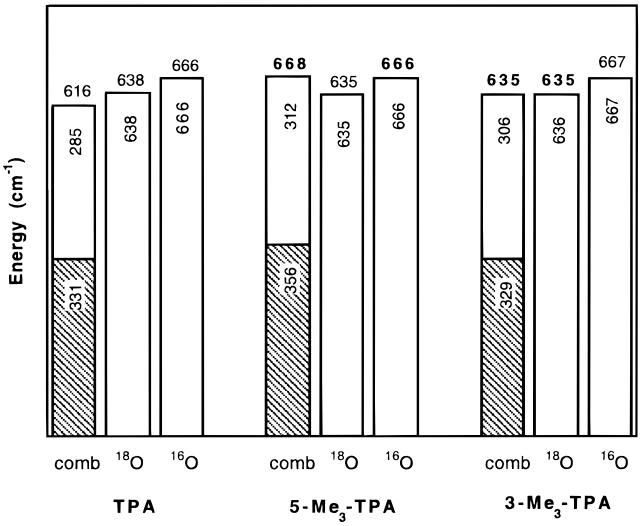

Figure 4. Graphical representation of transitions resulting (or not) in Fermi doublets in the 666 cm^{-1} band of $[Fe_2(\mu\text{-}O)_2(L)_2](ClO_4)_3$, where (A) L = TPA, (B) L = 5-Me_3-TPA, and (C) L = 3-Me_3-TPA, based on 1 cm^{-1} resolution data.

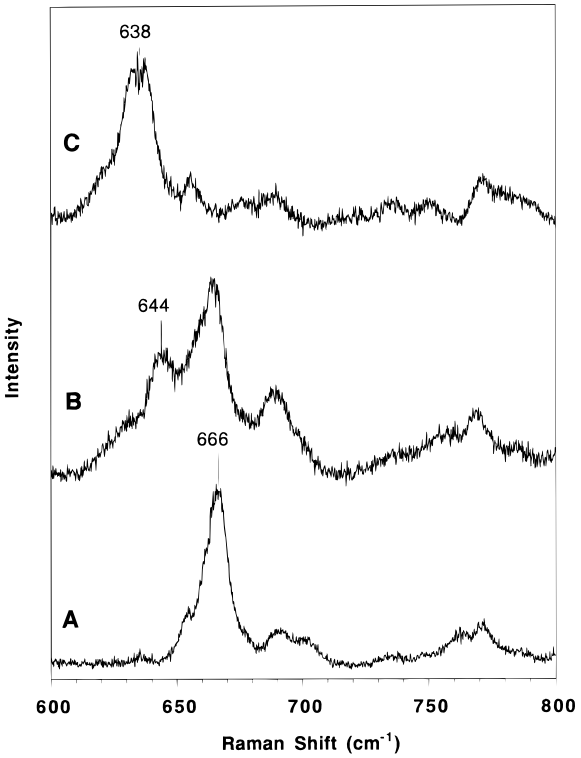

Figure 5. Resonance Raman spectra of 5 mM $[Fe_2(\mu\text{-}O)_2(TPA)_2](ClO_4)_3$ with (A) 300 equiv of $H_2{}^{16}O$ added, (B) 300 equiv of a 1:3 mixture of $H_2{}^{18}O/H_2{}^{16}O$ added, and (C) 300 equiv of $H_2{}^{18}O$ added.

must involve both oxygen atoms of the $Fe_2(\mu\text{-}O)_2$ diamond core. The $[Fe_2(\mu\text{-}O)_2(TPA)_2]^{3+}$ complex was chosen for this study because the absence of Fermi resonance effects in the 600−700 cm^{-1} region would best allow a feature of intermediate frequency to be observed. Thus, a sample of this complex prepared in the presence of 75:25 $H_2{}^{16}O/H_2{}^{18}O$ (Figure 5b) gives rise to a new peak at 644 cm^{-1}, intermediate between 666.1 and 637.9 cm^{-1}. This peak has an intensity indicating that it must arise from the complex with only one ^{18}O incorporated. Were the 666.1 cm^{-1} vibration associated with an Fe−O stretch or an Fe−O−Fe deformation, the mixed labeling experiment would produce only the peaks at 666.1 and 637.9 cm^{-1} and no feature at intermediate frequency. So the appearance of this feature at intermediate frequency demonstrates that the 666.1 cm^{-1} band arises from a vibration associated with the entire $Fe_2(\mu\text{-}O)_2$ diamond core. The 22 cm^{-1} isotope shift observed may appear larger than expected at first glance, but will be rationalized in a later section.

Another core vibration is observed in the lower frequency region of the Raman spectra of these complexes. $[Fe_2(\mu\text{-}O)_2(5\text{-}Me_3\text{-}TPA)_2]^{3+}$ exhibits an iron and oxygen isotope vibration at 409.1 cm^{-1}. This vibration too must involve motion of both oxygen atoms of the $Fe_2(\mu\text{-}O)_2$ core, as introduction of $H_2{}^{18}O$ results in the progressive appearance of new features at 402 and 394 cm^{-1}, corresponding to a shift of 7.1 and 15.1 cm^{-1}, respectively, for the singly- and doubly-labeled complex. The

corresponding features in the spectra of both $[Fe_2(\mu\text{-}O)_2(TPA)_2]^{3+}$ and $[Fe_2(\mu\text{-}O)_2(3\text{-}Me_3\text{-}TPA)_2]^{3+}$ exhibit similar isotope shifts upon complete exchange with $H_2{}^{18}O$ but are complicated by Fermi resonance with a metal−ligand mode. This metal−ligand mode is found at 426.5 cm^{-1} for the 5-Me_3-TPA complex and is sufficiently distinct from the 409.1 cm^{-1} diamond core vibration not to interact. However, the corresponding metal−ligand modes in the TPA and 3-Me_3-TPA complexes are closer in energy (408 and 405 cm^{-1}, respectively, as deduced from the ^{18}O data) and thus are in Fermi resonance with the ca. 409 cm^{-1} core vibration (Table 1).

Tripodal Ligand-Sensitive Vibrations. The 200−550 cm^{-1} region in the Raman spectra of the $[Fe_2(\mu\text{-}O)_2(TPA)_2](ClO_4)_3$ complexes is rich in features and can be divided into two groups of vibrations. The three low-intensity vibrations at 446, 473, and 514 cm^{-1} are somewhat sensitive to the iron isotope but relatively insensitive to alkyl substitutions on the tripodal ligand. Their modest resonance enhancement suggests that these vibrations do not follow along the same coordinates as the displacement in the electronic excited state; because of their low intensity, they will not be discussed further.

More interestingly, there are five vibrations between 200 and 430 cm^{-1} which are significantly affected by methyl substitution of the TPA ligand and are likely to arise from metal−ligand vibrations and/or tripodal ligand deformations. Since none of these vibrations shift with introduction of ^{15}N at the tertiary amine in the 5-Me_3-TPA ligand, it is unlikely that an $Fe-N_{amine}$ vibration is observed in these spectra. The vibrations observed are almost certainly metal−pyridine vibrations. Indeed features assigned as metal−ligand vibrations can be found in this region of the infrared spectra of transition metal (*viz.*, Co, Ni, Cu, and Zn) complexes of 3- and 4-alkylpyridines. For the vibrations of the $[Fe_2(\mu\text{-}O)_2(L)_2](ClO_4)_3$ complexes, there is no clear correlation between the energy of the vibration and the mass of the alkyl substituent. This is not surprising since it has been noted that the interaction of metal−ligand stretching with the pyridine−alkyl bending modes actually tends to oppose the simple mass effect (of adding the alkyl group).[15] Inspection of the spectra of the 5-Me_3-TPA complex show that the vibrations at 374 and 312 cm^{-1} are sensitive to iron isotope substitution, both exhibiting 4 cm^{-1} shifts between the ^{54}Fe and ^{58}Fe isotopomers, while the vibration at 254 cm^{-1} is iron-isotope-insensitive. While an exact assignment is not possible without a normal coordinate analysis that includes all the atoms of the pyridine, a number of symmetric and asymmetric combinations involving equatorial and axial pyridine moieties are possible on the basis of the geometry shown in Figure 1. The large isotope shifts exhibited by the 374 and 312 cm^{-1} modes are fully consistent with their assignment as Fe−Py stretching vibrations where the iron atom undergoes a net displacement, while the mode at 254 cm^{-1} is likely due to a symmetric stretch involving a collinear Py−Fe−Py unit.

$[Fe_2(\mu\text{-}O)_2]$ Core Vibration Assignments: Normal Coordinate Analysis. Since only recently have examples of an $Fe_2(\mu\text{-}O)_2$ diamond core become available in iron chemistry,[3] the data presented here represent all the available vibrational spectra for this type of complex. There are numerous examples of complexes containing the Fe−O−Fe unit, however. The vibrational spectra of these triatomic cores have been studied in great detail,[16] and the results from these studies can provide a starting point for understanding the vibrations of the $Fe_2(\mu\text{-}O)_2$ core. The C_{2v} Fe−O−Fe unit gives rise to three vibrations. As noted by Sanders-Loehr *et al.*,[16a] the symmetric Fe−O−Fe stretch (A_1 symmetry) is seen as a strong polarized band in the Raman spectrum in the region between 380 and 540 cm^{-1}, which decreases in energy as the Fe−O−Fe angle increases (Figure 6). The asymmetric Fe−O−Fe stretch (B_1 symmetry) is seen in the infrared spectrum (and sometimes in the Raman spectrum) in the region between 720 and 870 cm^{-1}, and the energy of the vibration increases as the Fe−O−Fe angle increases (Figure 6). The third vibration is an A_1 deformation that involves mainly a change in the Fe−O−Fe angle and is found (if seen at all) in the Raman spectrum at very low energy (ca. 100 cm^{-1}). The addition of the second oxo bridge to the Fe−O−Fe unit to form the $Fe_2(\mu\text{-}O)_2$ unit results in an Fe−O−Fe angle near 100°, much smaller than found for (μ-oxo)diiron(III) complexes. Nevertheless, the Fe−O vibrations at ca. 660−700 cm^{-1} observed for $[Fe_2(\mu\text{-}O)_2(6\text{-}Me_3\text{-}TPA)_2]^{2+}$ and the $[Fe_2(\mu\text{-}O)_2(3 \text{ or } 5\text{-}R_3\text{-}TPA)_2]^{2+}$ complexes (R = H or CH_3) fall in the region expected for (μ-oxo)diiron complexes when the correlations are extrapolated to smaller angles (Figure 6). In fact, the vibrations of the $Fe_2(\mu\text{-}O)_2$ complexes appear to correlate well with values associated with the asymmetric Fe−O−Fe mode. Though the mixed oxygen isotope data demonstrate that the 666 cm^{-1} feature is tetraatomic in nature, vibrations of the triatomic and the tetraatomic cores are clearly closely interrelated.

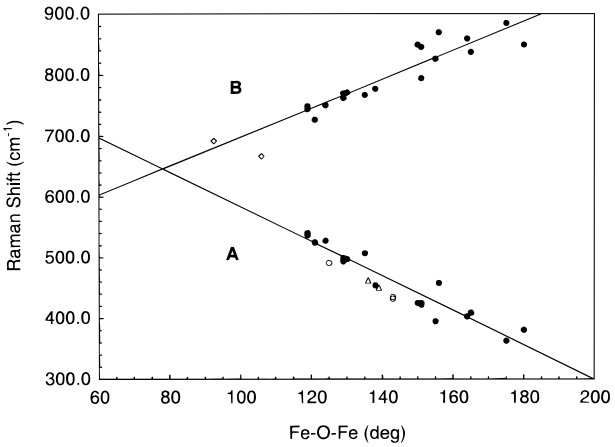

Figure 6. Correlation of the energy of (A) ν_{sym} and (B) ν_{asym} for a variety of complexes containing the Fe−O−Fe unit with the Fe−O−Fe angle. Data for $[Fe_2(\mu\text{-}O)_2(TPA)_2](ClO_4)_3$ and $[Fe_2(\mu\text{-}O)_2(6\text{-}Me_3\text{-}TPA)_2](ClO_4)_2$ diamond cores are indicated by diamond symbols. Data represented by solid circles are from ref 16a, open circles from ref 16c, and open triangles from ref 3b.

Symmetry analysis of this $[Fe_2(\mu\text{-}O)_2]^{3+}$ core in C_{2h} symmetry predicts six modes: two A_g (Raman-active) and two B_u (IR-active) modes that involve only Fe−O stretching, an A_u (IR-active) torsion or "butterfly" mode, and an A_g (Raman-active) mode that involves bending of the Fe−O−Fe and O−Fe−O angles. A normal coordinate analysis (NCA) of the $Fe_2(\mu\text{-}O)_2$ core was thus carried out using a geometry based on the EXAFS analysis of $[Fe_2(\mu\text{-}O)_2(5\text{-}Me_3\text{-}TPA)_2](ClO_4)_3$ as shown in Figure 1. The Fe−Fe distance of 2.89 Å and the short Fe−O distance of 1.77 Å come directly from the EXAFS analysis.[17] The longer Fe−O bond in the C_{2h} $Fe_2(\mu\text{-}O)_2$ core, which is presumably *cis* to the amine nitrogen as found in the X-ray structure of $[Fe_2(\mu\text{-}O)_2(6\text{-}Me_3\text{-}TPA)_2](ClO_4)_2$,[3a] could not be resolved from a

(15) Burgess, J. *Spectrochim. Acta* **1968**, *24A*, 277−283.

(16) (a) Sanders-Loehr, J.; Wheeler, W. D.; Shiemke, A. K.; Averill, B. A.; Loehr, T. M. *J. Am. Chem. Soc.* **1989**, *111*, 8084−8093. (b) Czernuszewicz, R. S.; Sheats, J. E.; Spiro, T. G. *Inorg. Chem.* **1987**, *26*, 2063−2067. (c) Holz, R. C.; Elgren, T. E.; Pearce, L. L.; Zhang, J. H.; O'Connor, C. J.; Que, L., Jr. *Inorg. Chem.* **1993**, *32*, 5844−5850.

(17) For details of the EXAFS analysis of $[Fe_2(\mu\text{-}O)_2(5\text{-}Me_3TPA)_2](ClO_4)_3$ the reader is referred to ref 3b.

Table 2. Data Used in Normal Mode Analysis of the $Fe_2(\mu\text{-}O)_2$ Core

internal coordinate	$Fe_2(\mu\text{-}O)_2$ core geometry	force constant[a]
bond stretch		K (stretching)
Fe1−O2 (r_1)	1.84	3.1509
Fe2−O2 (r_2)	1.77	3.1858
Fe1−O1 (r_3)	1.77	3.1858
Fe2−O1 (r_4)	1.84	3.1509
valence angle bending		H (bending)
Fe1−O1−Fe2 (α_1)	106.35	0.2115
Fe1−O2−Fe2 (α_2)	106.35	0.2115
O1−Fe1−O2 (α_3)	73.64	0.4104
O1−Fe2−O2 (α_4)	73.64	0.4104
		τ (torsion)
torsion angle[b] (τ_1)	180.0	0.3178
		F (sretch−stretch)
$r_1 + r_2$		0.2846
$r_3 + r_4$		0.2846
$r_1 + r_3$		0.0671
$r_2 + r_4$		0.0671
		F (stretch−bend)
$r_1 + \alpha_3$[b]		0.0754
$r_1 + \alpha_4$[c]		−0.0732

[a] K in mdyn/Å, H and τ in (mdyn·Å)/rad^2, F interaction constants in mdyn/Å. [b] $r_1 + \alpha_3 = r_2 + \alpha_3 = r_4 + \alpha_1 = r_3 + \alpha_1$. [c] $r_1 + \alpha_4 = r_2 + \alpha_2 = r_3 + \alpha_4 = r_4 + \alpha_2$.

shell of O/N scatterers with an average distance from the Fe of 1.94 Å. For the purpose of this analysis, we have assigned the longer bond a length of 1.84 Å, 0.07 Å longer than the 1.77 Å Fe−O bond. This bond length difference is commensurate with the 0.08 Å difference observed for $[Fe_2(\mu\text{-}O)_2(6\text{-}Me_3\text{-}TPA)_2](ClO_4)_2$[3a] and the 0.06 Å difference obtained from *ab initio* LDF−DFT calculations on the TPA analogue $[Fe_2(\mu\text{-}O)_2(TPA)_2]^{3+}$.[18] The calculated frequencies were not significantly changed when longer Fe−O bond lengths were used in the calculations.

Using the force field in Table 2, we calculated the six normal modes for the C_{2h} $Fe_2(\mu\text{-}O)_2$ core in $[Fe_2(\mu\text{-}O)_2(TPA)_2](ClO_4)_3$, and these modes, depicted with the displacement vectors generated by the atomic displacement matrix, are shown in Figure 7. The primary force constants used for the general valence force field (Table 2) are typical for an Fe−μ-O−Fe core,[16] with the addition of k_3 for the O−Fe−O bend and k_4 for the Fe_2O_2 torsion, both internal coordinates that are introduced by the addition of the second oxo bridge. The magnitude and sign of the interaction force constants were arrived at on the basis of previous calculations on the related $Mn_2(\mu\text{-}O)_2$ and the $Cu_2(\mu\text{-}\eta^2\text{:}\eta^2\text{-}O_2)$ cores.[19] The calculations using the force constants listed in Table 3 and the geometry shown in Figure 1 result in the frequencies listed in Table 3 for the six normal modes shown in Figure 7.

The prominent feature at around 666 cm^{-1} found in all the $[Fe_2(\mu\text{-}O)_2]^{3+}$ complexes is sensitive only to the introduction of Fe and O isotopes. It must arise from one of the two A_g stretching modes of the $Fe_2(\mu\text{-}O)_2$ core, ν_2 or ν_3, both of which are calculated to have frequencies in the 600−700 cm^{-1} region, with the $^{54}Fe/^{58}Fe$, $^{54}Fe/^{57}Fe$, and $^{16}O_2/^{18}O_2$ isotope shifts listed in Table 2. The $^{54}Fe/^{58}Fe$ and $^{16}O_2/^{18}O_2$ isotopic shifts for the 666.2 cm^{-1} band of $[Fe_2(\mu\text{-}O)_2(5\text{-}Me_3\text{-}TPA)_2]^{3+}$ are −2.5 and −31.2 cm^{-1}, respectively, values which agree better with the isotope shifts calculated for ν_2 (Table 2). Because the 666.2 cm^{-1} band of $[Fe_2(\mu\text{-}O)_2(5\text{-}Me_3\text{-}TPA)_2]^{3+}$ appears as a Fermi doublet, its isotope shifts may be difficult to measure accurately, so the analogous isotope shift study was carried out on $[Fe_2(\mu\text{-}O)_2(TPA)_2]^{3+}$, which exhibits a single peak at 666.1 cm^{-1}. This feature shows $^{54}Fe/^{57}Fe$ and $^{16}O_2/^{18}O_2$ isotope shifts of −3.7 and −28.2 cm^{-1}, respectively, values similar to those observed for $[Fe_2(\mu\text{-}O)_2(5\text{-}Me_3\text{-}TPA)_2]^{3+}$. These shifts can be associated with ν_2 or ν_3 but are more consistent with the ν_2 assignment.

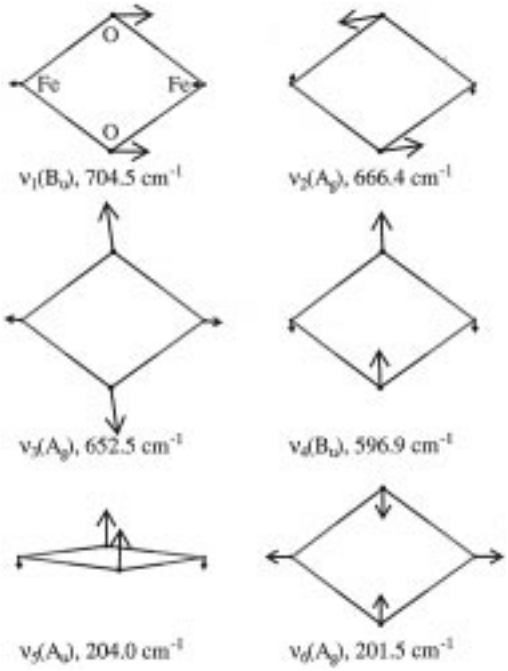

Figure 7. Atomic displacement vectors for the normal modes calculated for $[Fe_2(\mu\text{-}O)_2(5\text{-}Me_3\text{-}TPA)_2](ClO_4)_3$.

Where then is the other A_g stretching mode ν_3? Closer examination of the 600−700 cm^{-1} region of the spectrum of $[Fe_2(\mu\text{-}O)_2(TPA)_2]^{3+}$ reveals a shoulder on the low-frequency side of the 666.1 cm^{-1} feature. This shoulder at 655.3 cm^{-1} exhibits $^{54}Fe/^{57}Fe$ and $^{16}O_2/^{18}O_2$ isotope shifts of −3.2 and −32.6 cm^{-1}. Given the similarities in their Fe and O isotope shifts, the 666.1 and 655.3 cm^{-1} features cannot be unequivocally assigned to either ν_2 or ν_3. One way to resolve this puzzle is to consider the $^{16}O_2/^{16}O^{18}O$ isotope shift. The calculations show that the mixed isotope shifts differ significantly for ν_2 and ν_3, −21.3 vs −11.2 cm^{-1}. The $^{16}O^{18}O$ derivative of $[Fe_2(\mu\text{-}O)_2(TPA)_2]^{3+}$ shows a peak at 644 cm^{-1}. This corresponds to an isotope shift of −22.1 cm^{-1} relative to the 666.1 cm^{-1} feature and −11.3 cm^{-1} from the 655.3 cm^{-1} shoulder, thus making it possible that both peaks are superimposed at 644 cm^{-1} in the $^{16}O^{18}O$ spectrum. This result supports an assignment of the 666.1 cm^{-1} peak to ν_2 and the 655.3 cm^{-1} feature to ν_3.

An interesting question to discuss is why ν_2 should be more prominent than ν_3. In triatomic Fe−O−Fe complexes, the more intense feature usually arises from the symmetric stretch; this vibration corresponds to ν_3 of the $Fe_2(\mu\text{-}O)_2$ core, the core breathing mode where all Fe−O bonds stretch in phase. ν_2 for the $Fe_2(\mu\text{-}O)_2$ core corresponds to the asymmetric stretch of the Fe−O−Fe complexes which is usually quite weak in the Raman spectrum. Exceptions arise when the Fe−O−Fe unit exhibits some asymmetry. Indeed there are two examples where the asymmetric stretch is the most prominent feature in the Raman spectrum, $[Cl_3Fe{-}O{-}FeN5]^{+}$[20] and $[Fe_2(\mu\text{-}O)(\mu\text{-}O_2C^tBu)_2(Me_3\text{-}TACN)_2]^{+}$.[21] For these two complexes, there is a significant difference in the lengths of the two Fe−μ-O bonds which leads to enhancement of the asymmetric stretch and the corresponding

(18) Ghosh, A.; Almlöf, J.; Que, L., Jr. *Angew. Chem., Int. Ed. Engl.* **1996**, *35*, 770−772.
(19) Ling, J.; Nestor, L. P.; Czernuszewicz, R. S.; Spiro, T. G.; Fraczkiewicz, R.; Sharma, K. D.; Loehr, T. M.; Sanders-Loehr, J. *J. Am. Chem. Soc.* **1994**, *116*, 7682−7691.

Table 3. Calculated Frequencies and Isotope Shifts (cm^{-1}) for Vibrations of the $Fe_2(\mu\text{-}O)_2$ Core in $[Fe_2(\mu\text{-}O)_2(5\text{-}R_3\text{-}TPA)_2](ClO_4)_3$

assignment	frequency	$\Delta(^{18}O)_2$[a]	$\Delta(^{18}O)(^{16}O)$[a]	$\Delta^{54}Fe/^{58}Fe$[a]	$\Delta^{54}Fe/^{57}Fe$[a]	PED (%)[b]
Calculated for the C_{2h} $[Fe_2(\mu\text{-}O)_2]$ Core						
ν_1 (B_u)	704.5	−31.1	−9.9	5.6	4.3	r_1 (58), r_2 (54), $r_1 + r_2$ (−10)
ν_2 (A_g)	666.4	−32.5	−21.3	3.4	2.6	r_1 (70), r_2 (41), $r_1 + r_2$ (−10)
ν_3 (A_g)	652.5	−27.1	−11.2	6.2	4.8	r_1 (58), r_2 (28), $r_1 + r_2$ (7)
ν_4 (B_u)	596.9	−26.4	−16.2	4.7	3.6	r_1 (46), r_2 (42), $r_1 + r_2$ (8), α_1 (6)
ν_5 (A_u)	204.0	−9.0	−4.5	1.6	1.2	τ_1 (100)
ν_6 (A_g)	210.5	−3.4	−1.7	5.2	4.0	α_3 (63), α_1 (32)
Observed for $[Fe_2(\mu\text{-}O)_2(5\text{-}Me_3\text{-}TPA)_2](ClO_4)_3$						
ν_2 or ν_3	666.2	−31.2	not resolved	2.5		
$2\nu_5$[a]	409.1	−15.1	−7.1	6.2		
Observed for $[Fe_2(\mu\text{-}O)_2(TPA)_2](ClO_4)$						
ν_2 (or ν_3)	666.1	−28.2	−22.1		3.7	
ν_3 (or ν_2)	655.3	−32.6	not found		3.2	

[a] $\Delta(^{18}O)_2 = \nu(^{18}O)_2 - \nu(^{16}O)_2$; $\Delta(^{18}O)(^{16}O) = \nu(^{18}O)(^{16}O) - \nu(^{16}O)_2$, $\Delta^{54}Fe/^{58}Fe = \nu(^{54}Fe) - \nu(^{58}Fe)$, $\Delta^{54}Fe/^{57}Fe = \nu(^{54}Fe) - \nu(^{57}Fe)$. [b] Potential energy distributions calculated with respect to force constants.[31] Symbols correspond to those in Table 2.

decrease in intensity of the symmetric stretch. The fact that the Fe−μ-O bonds of each Fe−O−Fe unit of the $Fe_2(\mu\text{-}O)_2$ core have different lengths, i.e., C_{2h}, rather than D_{2h}, symmetry, rationalizes the enhancement of the ν_2 mode relative to the ν_3 mode.

The only other feature that is sensitive as well to Fe and O isotopes is at 409.1 cm^{-1} in the spectrum of $[Fe_2(\mu\text{-}O)_2(5\text{-}Me_3\text{-}TPA)_2]^{3+}$. This feature appears as a Fermi doublet in the spectra of the TPA and 3-Me_3-TPA analogs and is thus more difficult to interpret in the latter complexes. The $^{54}Fe/^{58}Fe$ and $^{16}O_2/^{18}O_2$ isotope shifts observed for the 5-Me_3-TPA complex are 6.2 and 15.1 cm^{-1}, respectively. A perusal of Table 3 shows no A_g mode near 400 cm^{-1}. However, the first overtone of ν_5, the out-of-plane butterfly motion of the core (A_u symmetry), which is calculated to appear at 204.0 cm^{-1}, would afford a band at the right energy and with appropriate isotope shifts. Significant resonance enhancement of the first overtone of the IR-active out-of-phase breathing mode of the two linked FeS_4 tetrahedra has also been observed in the Raman spectra of model $Fe_2(\mu\text{-}S)_2$ complexes.[22] We thus assign the 409.1 cm^{-1} band as $2\nu_5$, the first overtone of ν_5.

Conclusion

Resonance Raman spectra of complexes containing the high-valent $Fe_2(\mu\text{-}O)_2$ diamond core all show an oxygen- and iron-isotope-sensitive vibration centered around 666 cm^{-1}. This vibration is unique to this type of complex, and through isotope substitution, ligand substitution, and normal coordinate analysis, we assign this vibration as ν_2, the A_g mode of the C_{2h} $Fe_2(\mu\text{-}O)_2$ core which involves stretching of the two shorter Fe−O bonds alternating with stretching of the two longer Fe−O bonds (Figure 7). A strongly resonance-enhanced, oxygen-isotope-sensitive vibration between 600 and 700 cm^{-1} is also observed for the diiron(III) complex $[Fe_2(\mu\text{-}O)_2(6\text{-}Me_3\text{-}TPA)_2](ClO_4)_2$ as well as for complexes with $Mn_2(\mu\text{-}O)_2$[11] and $Cu_2(\mu\text{-}O)_2$ cores.[4] Taken together, these data indicate that a 600−700 cm^{-1} band with significant oxygen isotope sensitivity is a characteristic feature of the Raman spectra of complexes containing the $M_2(\mu\text{-}O)_2$ diamond core. An $Fe_2(\mu\text{-}O)_2$ diamond core has been proposed[7] as one of the structures for the high-valent intermediates **Q** and **X** in the redox cycles of methane monooxygenase[9,23] and ribonucleotide reductase,[24] respectively. Resonance Raman spectroscopy would thus be a useful tool to probe the structures of such intermediates and ascertain whether such a diamond core is involved in the catalytic cycle of nonheme diiron enzymes.

Experimental Section

General Procedures. All reagents and solvents were obtained from commercial sources and used as received unless otherwise noted. Oxygen isotope $H_2{}^{18}O$ (98% enriched) and iron isotopes $^{54}Fe_2O_3$ (99.9% enriched), $^{57}Fe_2O_3$ (99.9% enriched), and ^{58}Fe (89% enriched) were obtained from commercial sources and used as received. Solvents were dried according to published procedures.[25] *Caution! The perchlorate salts in this study are all potentially explosive and should be handled with care.*

Tris(3-methyl-2-pyridylmethyl)amine (3-Me_3-TPA). A mixture of 4.85 g (24.8 mmol) of 2-(aminomethyl)-3-methylpyridine hydrochloride (prepared as described by Dong et al.[3a]) and 8.83 g (49.5 mmol) of 2-(chloromethyl)-3-methylpyridine hydrochloride (prepared as described by Hardegger[26] and Baker et al.[27]) in 30 mL of water was neutralized with 5.1 g (127.5 mmol) of NaOH in 10 mL of water at 0 °C. This solution was stirred at room temperature for 2 days, at the end of which solid product (7.2 g) precipitated in 92% yield. The solid was dissolved in $CHCl_3$, and the solution was washed with water. The purified product (5.0 g, 64% yield) was precipitated from the $CHCl_3$ solution with ether. ^1H NMR ($CDCl_3$): δ (ppm) 1.65 (s, 3H, $-CH_3$), 3.84 (s, 2H, CH_2N), 7.09 (dd, 1H, β-pyr), 7.33, (d, 1H, α- or γ-pyr), 8.38 (d, 1H, α- or γ-pyr).

***N*,*N*-Bis(5-methyl-2-pyridylmethyl)-*N*-(2-pyridylmethyl)ammonium Perchlorate (5-Me_2-TPA·3HClO$_4$).** A mixture of 0.61 g (5.6 mmol) of 2-(aminomethyl)pyridine and 2.00 g (11.2 mmol) of 2-(chloromethyl)-5-methylpyridine hydrochloride in 10 mL water was neutralized with 0.90 g (22.5 mmol) of NaOH in 5 mL of water at 0 °C. This solution was stirred at room temperature for 3 days and extracted with CH_2Cl_2. The extract was washed with water, and the solvent was

(20) Gomez-Romero, P.; Witten, E. H.; Reiff, W. M.; Backes, G.; Sanders-Loehr, J.; Jameson, G. B. *J. Am. Chem. Soc.* **1989**, *111*, 9039−9047.

(21) Cohen, J. D.; Payne, S.; Hagen, K. S.; Sanders-Loehr, J. *J. Am. Chem. Soc.* **1997**, *119*, 2960−2961.

(22) Han, S.; Czernuszewicz, R. S.; Spiro, T. G. *J. Am. Chem. Soc.* **1989**, *111*, 3496−3504.

(23) (a) Lee, S.-K.; Nesheim, J. C.; Lipscomb, J. D. *J. Biol. Chem.* **1993**, *268*, 21569−21577. (b) Lee, S.-K.; Fox, B. G.; Froland, W. A.; Lipscomb, J. D.; Münck, E. *J. Am. Chem. Soc.* **1993**, *115*, 6450−6451. (c) Liu, K. E.; Valentine, A. M.; Wang, D.; Huynh, B. H.; Edmondson, D. E.; Salifoglou, A.; Lippard, S. J. *J. Am. Chem. Soc.* **1995**, *117*, 10174−10185.

(24) (a) Riggs-Gelasco, P. J.; Shu, L.; Chen, S.; Burdi, D.; Huynh, B. H.; Que, L., Jr.; Stubbe, J. *J. Am. Chem. Soc.*, in press. (b) Sturgeon, B. E.; Burdi, D.; Chen, S.; Huynh, B.-H.; Edmondson, D. E.; Stubbe, J.; Hoffman, B. M. *J. Am. Chem. Soc.* **1996**, *118*, 7551−7557. (c) Bollinger, J. M., Jr.; Edmondson, D. E.; Huynh, B. H.; Filley, J.; Norton, J.; Stubbe, J. *Science (Washington, D.C.)* **1991**, *253*, 292−298.

(25) Perrin, D. D.; Armarego, W. L. F. *Purification of Laboratory Chemicals*; Pergamon Press: New York, 1988.

(26) Hardegger, E.; Nikles, E. *Helv. Chim. Acta* **1957**, *40*, 2428−2433.

(27) Baker, W.; Buggle, K. M.; McOmie, J. F. W.; Watkins, D. A. M. *J. Chem. Soc. London* **1958**, 3594−3603.

evaporated in *vacuo*. The residue was treated with concentrated $HClO_4$, and the light yellow product (2.6 g, 74%) was precipitated from the acetone solution with ether. ^{1}H NMR (D_2O): δ (ppm) 2.48 (s, 6H, $-CH_3$), 4.31 (s, 4H, CH_2N of 5-Me-py), 4.35 (s, 2H, CH_2N of py), 7.91−7.99 (m, 3H), 8.06−8.10 (d, 1H), 8.32−8.36 (d, 2H), 8.50−8.55 (m, 3H), 8.71−8.74 (d, 1H).

***N*-(5-Methyl-2-pyridylmethyl)-*N*,*N*-bis(2-pyridylmethyl)ammonium Perchlorate (5-Me-TPA·3HClO$_4$).** A mixture of 1.17 g (5.9 mmol) of bis(2-pyridylmethyl)amine and 1.05 g (5.9 mmol) of 2-(chloromethyl)-5-methylpyridine hydrochloride in 10 mL water was neutralized with 0.47 g (11.8 mmol) of NaOH in 5 mL of water at 0 °C. This solution was stirred at room temperature for 3 days and extracted with CH_2Cl_2. The extract was washed with water, and the solvent was evaporated in *vacuo*. The residue was treated with concentrated $HClO_4$, and the light yellow product (2.9 g, 81%) was precipitated from the acetone solution with ether. ^{1}H NMR (D_2O): δ (ppm) 2.45 (s, 3H, $-CH_3$), 4.30 (s, 2H, CH_2N of 5-Me-py), 4.34 (s, 4H, CH_2N of py), 7.89−7.96 (m, 3H), 8.03−8.07 (d, 2H), 8.28−8.32 (d, 1H), 8.44−8.52 (m, 3H), 8.68−8.71 (d, 2H).

[Fe$_2$O(3-Me$_3$-TPA)$_2$(OH)(H$_2$O)](ClO$_4$)$_3$ was prepared by mixing ligand (0.95 mmol) and Et_3N (3.10 mmol) in 20 mL of methanol and $Fe(ClO_4)_3\cdot 10H_2O$ (0.500 g, 0.94 mmol) in 5 mL of methanol. The solution was allowed to stand on the bench for 1 day, and dark green crystals formed which were filtered. Anal. Calcd for [Fe$_2$O(3-Me$_3$-TPA)$_2$(OH)(H$_2$O](ClO$_4$)$_3\cdot 2H_2O$ ($C_{42}H_{55}Cl_3Fe_2N_8O_{17}$): C, 43.41; H, 4.77; N, 9.64. Found: C, 43.62, H, 4.69, N, 9.36.

[Fe$_2$O(5-Me$_2$-TPA)$_2$(OH)(H$_2$O)](ClO$_4$)$_3$ and [Fe$_2$O(5-Me-TPA)$_2$-(OH)(H$_2$O)](ClO$_4$)$_3$ were prepared by mixing ligand HCL salt (0.94 mmol) and Et_3N (4.5 mmol) in 20 mL of methanol and $Fe(ClO_4)_3\cdot 10H_2O$ (0.500 g, 0.94 mmol) in 5 mL of methanol. The solution was allowed to stand on the bench for 1 day, and dark green crystals formed which were filtered. Anal. Calcd for [Fe$_2$O(5-Me$_2$-TPA)$_2$(OH)-(H$_2$O)](ClO$_4$)$_3\cdot 2H_2O$ ($C_{40}H_{51}Cl_3Fe_2N_8O_{17}$): C, 42.36; H, 4.53; N, 9.88. Found: C, 42.33, H, 4.79, N, 9.28. Anal. Calcd for [Fe$_2$O(5-Me-TPA)$_2$(OH)(H$_2$O)](ClO$_4$)$_3\cdot 2H_2O$ ($C_{38}H_{47}Cl_3Fe_2N_8O_{17}$): C, 41.27; H, 4.28; N, 10.13. Found: C, 41.22, H, 4.17, N, 10.07.

Samples. [Fe$_2$(μ-O)$_2$(6-Me$_3$-TPA)$_2$](ClO$_4$)$_2$ was prepared according to the published procedures.[3a] ^{54}Fe and ^{58}Fe samples of [Fe$_2$(μ-O)$_2$(5-Me$_3$-TPA)$_2$](ClO$_4$)$_3$ and ^{54}Fe and ^{57}Fe samples of [Fe$_2$(μ-O)$_2$(TPA)$_2$]-(ClO$_4$)$_3$ were prepared according to the procedure for preparation of ^{57}Fe samples.[3b] Samples of [Fe$_2$(μ-O)$_2$L$_2$](ClO$_4$)$_3$ (L = 3-Me$_3$-TPA or 5-Me$_3$-TPA) were prepared by dissolving the pure solid (prepared according to the published procedure)[3b] in a vial of CH_3CN that is suspended in a −40 °C bath. All other samples of [Fe$_2$(μ-O)$_2$L$_2$](ClO$_4$)$_3$ were prepared by dissolving the starting material [Fe$_2$(μ-O)(OH)-(H$_2$O)L$_2$](ClO$_4$)$_3$ in a vial of CH_3CN, placing the vial in a −40 °C bath, and adding 1.5 equiv of H_2O_2 to generate the [Fe$_2$(μ-O)$_2$L$_2$](ClO$_4$)$_3$ complex.

Raman Spectroscopy. Raman spectra were recorded at the University of Minnesota on a Spex 1403 double spectrometer interfaced with a Spex DM3000 data system using a Spectra Physics 2030-15 argon ion laser, and a 375B CW dye (Rhodamine 6G) laser. Spectra were obtained at 77 K using a back-scattering geometry, and Raman frequencies are referenced to appropriate solvent features that were in turn calibrated with neon and mercury discharge lamps. Samples were frozen onto a gold-plated copper cold finger in thermal contact with a dewar containing liquid nitrogen.[28] All spectra were recorded with slits set for a band-pass of 2 cm^{-1}. Most spectra were obtained with scan increments of 1 cm^{-1}, and peak positions are listed to 1 cm^{-1} precision. A protocol reported by Nakamoto was used to obtain peak positions reported to 0.1 cm^{-1} precision,[29] which entailed averaging four highly reproducible scans with scan increments of 0.1 cm^{-1}. To calculate the peak positions, the region of interest was expanded, the peaks fit with a Voigtian line shape, and the centroid taken as the peak frequency.

Normal Coordinate Analysis. Normal mode calculations were carried out with the **GF** matrix method[30] and a general valence force field which included bond stretching, angle bending, and torsional force constants. Also included were valence interaction force constants for all coordinates sharing at least one atom. All calculations were carried out on a Silicon Graphics INDY workstation using a UNIX version of the RAMVIB software.[31] The visualization of normal eigenvectors was accomplished by transfer of the Cartesian atomic displacements into the X-Mol molecular graphics program.[32] Molecular parameters for the Fe$_2$(μ-O)$_2$ unit of [Fe$_2$(μ-O)$_2$(5-Me$_3$-TPA)$_2$](ClO$_4$)$_3$ were obtained from bond distances determined by EXAFS,[3b] from which the Cartesian coordinates were determined by simple trigonometric relationships.

Acknowledgment. We thank the National Institutes of Health for grants (GM33162 to L.Q. and GM48370 to R.S.C.) and a predoctoral traineeship (GM07323 to E.C.W.) in support of this work.

JA973220U

(28) Czernuszewicz, R. S.; Johnson, M. K. *Appl. Spectrosc*. **1983**, *37*, 297−298.
(29) Nakamoto, K. *Angew. Chem., Int. Ed. Engl.* **1972**, *11*, 666−674.
(30) Wilson, E. B.; Decius, J. C.; Cross, P. C. *Molecular Vibrations*; McGraw-Hill: New York, 1955.
(31) Fraczkiewicz, R.; Czernuszewicz, R. S. *J. Mol. Struct.* **1997**, *435*, 109−121.
(32) *X-Mol*, version 1.3.1; Minnesota Supercomputer Center, Inc.: Minneapolis, MN, 1993.